Technical Note: Estimating light-use efficiency of benthic habitats using underwater O₂ eddy covariance

Karl M. Attard[1, 2] & Ronnie N. Glud[1, 3]

[1]Department of Biology, University of Southern Denmark, Odense, 5230, Denmark
5   [2]Tvärminne Zoological Station, University of Helsinki, Hanko, 10900, Finland
[3]Department of Ocean and Environmental Sciences, Tokyo University of Marine Science and Technology, Tokyo, Japan

Correspondence to: Karl M. Attard (karl.attard@biology.sdu.dk)

0.   Abstract

10   Light-use efficiency defines the ability of primary producers to convert sunlight energy to primary production and is computed as the ratio between the gross primary production and the intercepted photosynthetic active radiation. While this measure has been applied broadly within the atmospheric sciences to investigate resource-use efficiency in terrestrial habitats, it remains underused within the aquatic realm. This report provides a conceptual framework to compute hourly and daily light-use
15   efficiency using underwater O₂ eddy covariance, a recent technological development that produces habitat-scale rates of primary production under unaltered in situ conditions. The analysis, tested on two flux datasets, documents that hourly light-use efficiency may approach the maximum theoretical limit of 0.125 O₂ photon^{-1} under low light conditions but it decreases rapidly towards the middle of the day and is typically an order of magnitude lower on a 24 h basis. Overall, light-use efficiency provides a
20   useful measure of habitat functioning and facilitates site comparison in time and space.

1. Introduction

1.1 Eddy covariance estimates of benthic primary production

Underwater eddy covariance (EC) is a recent technological development that has emerged as an
25   important tool in benthic primary production studies. One of its key attributes is that it generates benthic O₂ fluxes at a high temporal resolution (typically ~15 min) over several days, and it does so for large seafloor areas (10s of m², i.e. on a habitat-scale) and under unaltered *in situ* conditions (Berg et al.,

2007;Berg et al., 2017). Eddy covariance thus overcomes many of the limitations of traditional methods (e.g. chamber incubations) and enables primary production rates to be measured within a wide range of benthic habitats (Chipman et al., 2016;Hume et al., 2011;Long et al., 2013;Volaric et al., 2018;Attard et al., 2019b). Additionally, the EC method can resolve very small benthic fluxes down to ~1 mmol O_2 m^{-2}

5 d^{-1} or less (Berg et al., 2009;Donis et al., 2016), which allows reliable measurements of primary production to be made in low-activity benthic settings, such as in high-latitude environments in winter and in deep phototrophic communities (Attard et al., 2014;Attard et al., 2016).

1.2 Constraining hourly and daily *GPP*

Sources of variability within EC O_2 fluxes can be broadly grouped into two categories, namely (1)

10 sources that bias the measured EC flux away from the 'true' benthic flux (i.e. when EC O_2 flux $\neq$ benthic O_2 flux) due to e.g. non-steady state conditions within the benthic boundary layer and (2) 'true' temporal variability in the benthic O_2 exchange rate (i.e. when EC O_2 flux = benthic O_2 flux) due to e.g. flow-induced advective pore water exchange in highly permeable sediments (Table 1). Despite there being numerous sources of variability, high-quality EC fluxes often show a tight coupling to sunlight

15 (photosynthetic active radiation, *PAR*) availability on the hourly timescale, indicating a dominant primary production signal in many aquatic systems (Berg et al., 2013;Chipman et al., 2016;Attard et al., 2014;Attard et al., 2015;Rheuban et al., 2014;Long et al., 2013;Long et al., 2015;Koopmans et al., 2020;Rovelli et al., 2017).

Under ideal conditions, the measured EC fluxes represent the balance between habitat *GPP* and *R*.

20 Hourly and daily *GPP* may therefore be computed from the EC fluxes by offsetting daytime fluxes by the dark *R* rate, as $GPP = FLUX_{day} + \left| \overline{FLUX_{night}} \right|$. It is well known that this approach provides

conservative estimates of *GPP*, since *R* typically is higher during daytime in the presence of

photosynthesis (Fenchel and Glud, 2000;Hotchkiss and Hall, 2014). Indeed, several EC studies have

documented lower O_2 effluxes in the evening than in the morning under similar light intensities (a so-

called 'hysteresis'), and high *R* rates at the onset of darkness (Rovelli et al., 2017;Rheuban et al.,

5 2014;Koopmans et al., 2020). It is generally understood that *R* is stimulated by *GPP*; it increases

progressively throughout the day as labile photosynthates accumulate (Epping and Jørgensen, 1996;de

Winder et al., 1999), and the magnitude of the hysteresis is related to the light history (Adams et al.,

2016). While it is highly relevant to quantify daytime *R*, direct measurements are usually not available.

1.3 Light-use efficiency

10 Gross primary production can be formulated as the product of incident *PAR*, the fraction of absorbed

PAR (*fAPAR*), and the light-use efficiency (*LUE*), that is $GPP = PAR * fAPAR * LUE$ (Monteith et al.,

1977). The *LUE* indicates the efficiency with which absorbed *PAR* is converted to *GPP*. This approach

has been applied broadly within the atmospheric sciences to investigate crop yield, productivity and

resource-use efficiency among terrestrial biomes using eddy covariance flux tower data (Stocker et al.,

15 2018;Hemes et al., 2020). In aquatic environments, the *LUE* has been applied primarily on the

microscale to investigate energy budgets of photosynthetic microbial mats and symbiont-bearing corals

(Al-Najjar et al., 2010;Al-Najjar et al., 2012;Brodersen et al., 2014). These detailed measurements have

revealed that most (> 80 %) of the incident solar energy is dissipated as heat, and conservation by

photosynthesis typically is < 5 %. Despite low energy utilization, some benthic ecosystems such as

20 coral reef symbionts seem particularly efficient at converting *PAR* to *GPP*, with *LUE* approaching the

theoretical limit of 8 mol photons of *PAR* required to produce 1 mol of O_2 through *GPP* (0.125 O_2

photon $^{-1}$) (Brodersen et al., 2014). To our knowledge there is one study using chamber incubations that employs the *LUE* approach to investigate benthic primary production in lakes (Godwin et al., 2014), and this remains unexplored within underwater EC studies. Since the *EC* method can produce hourly and daily *GPP* measurements across many different habitat types (Attard et al., 2019b), applying the

5   *LUE* approach could provide a useful measure of the efficiency with which solar energy is converted to *GPP* on the spatial scale of whole habitats. A key requirement for computing the *LUE* is to have reliable estimates of *GPP*. In this report we will therefore aim to provide a conceptual framework for computing hourly *GPP* from EC fluxes, and from this, compute the *LUE*. We then test this approach on measured EC flux data.

10   **2.   Materials and methods**

2.1 Eddy covariance data

This study uses a four day long EC data from Attard et al. (2014) and a three day long dataset from Attard et al. (in review). Attard et al. (2014) performed seasonal measurements at subtidal (3-22 m depth) light-exposed benthic habitats in a sub-Arctic fjord in Greenland, whereas Attard et al. (in

15   review) conducted their seasonal study on a 5 m deep mussel reef in the Baltic Sea. Two flux datasets were selected from these two studies to represent datasets with and without flux hysteresis. Instrument setup and data processing is described in detail in these papers. In short, the EC instrumentation consisted of a single-point acoustic velocimeter (Vector, Nortek), a fast-response O_2 microsensor setup (McGinnis et al., 2011), and a downwelling cosine *PAR* sensor (QCP-2000, Biospherical Instruments or

20   LI-192, Li-Cor) mounted onto the frame. The instrument was deployed from a small research vessel and was left to collect data over several days. Benthic O_2 fluxes were extracted for consecutive 10- or 15-

min periods using the software package SOHFEA (McGinnis et al., 2014), and the fluxes were bin-averaged to 1 h for interpretation.

2.2 Computing hourly *GPP*

2.2.1 Defining a daytime R rate

5   Time series of EC fluxes were split into individual 24 h sections representing periods from midnight to midnight. Each 24 h time series was aligned with corresponding seabed *PAR* data. Daytime periods were defined as periods when $PAR > 2.0$ µmol m^{-2} s^{-1}. Each 24 h section therefore had two night-time periods- the first from midnight to sunrise (N_1), and the second from sunset to midnight (N_2). Four options for computing the daytime R rate were explored. The first two approaches assumed a static R

10   rate during the day whereas the third and fourth approaches assumed dynamic (time-variable) daytime R. In the first approach, daytime fluxes were offset by $|\overline{N_1}|$ and in the second approach, daytime R was defined as an average of N_1 and N_2 fluxes ($|\overline{N_1 + N_2}|$). These two approaches are expected to work best when O_2 fluxes do not show a hysteresis. However, for other datasets that do show substantial hysteresis, this approach might underestimate R (and therefore GPP) in the second half of the day. The

15   third and fourth approach attempted to correct for this by assuming a dynamic hourly daytime R rate that increases progressively throughout the day. The third approach assumed a linear increase in hourly daytime R with time from $|\overline{N_1}|$ to $|\overline{N_2}|$, whereas the fourth approach assumed a sigmoidal increase with time from $|\overline{N_1}|$ to $|\overline{N_2}|$ in concert with changes in seabed *PAR*. To calculate the shape of the sigmoidal curve for this fourth approach, the *PAR* time series was integrated over time and the resultant data were

20   fitted with a sigmoidal (Boltzmann) function as:

$$\int_0^{24} PAR\,(t) = A_2 + (A_1 - A_2)/(1 + \exp\left(\frac{PAR - x_0}{dx}\right))$$

where A_1 and A_2 were the initial and final PAR values, x_0 is the centre of the curve, and dx is a time

constant. This function gave very tight fits to the integrated PAR data ($R^2 > 0.99$). The fitting parameters

x_0 and dx were then used to define the sigmoidal increase in daytime respiration from A_1 to A_2 ($|\overline{N_1}|$ to

$|\overline{N_2}|$). Hourly daytime R rates were computed using this approach, and then summed with their

corresponding measured daytime flux to compute the GPP.

2.2.2 Light-saturation curves

The ability of the four approaches to produce reliable estimates of hourly GPP was evaluated using

light-saturation curves. Several mathematical formulations are available to investigate photosynthetic

performance (Jassby and Platt, 1976), but benthic studies typically use linear regression or the

tangential hyperbolic function by Platt et al. (1980):

$$GPP = P_m * \tanh\left(\frac{\alpha I}{P_m}\right)$$

where P_m is the maximum rate of benthic gross primary production (in mmol O_2 m^{-2} h^{-1}), I is the near-

bed irradiance (PAR; in µmol photons m^{-2} s^{-1}), and α is the quasi-linear initial slope of the curve (mmol

O_2 m^{-2} h^{-1} [µmol PAR m^{-2} s^{-1}]). From these curves it is possible to derive the photoadaptation parameter

I_k (µmol PAR m^{-2} s^{-1}) as $I_k = P_m/\alpha$. If we assume that hourly benthic GPP is predominantly driven by

PAR, then high-quality light saturation curves for GPP should (a) show a high correlation with PAR

(high R^2 value), and (b) have a low standard error for the fitting parameters P_m, α, and I_k. High-quality

hourly GPP values should also be non-negative. Non-linear curve fitting was performed in OriginPro

2020 using a Levenberg-Marquardt iteration algorithm, and the standard error of the fitting parameters was scaled with the square root of reduced chi-squared statistic.

2.3 Estimating light-use efficiency

2.3.1 Constraining the fraction of absorbed PAR (fAPAR)

5 Direct measurements of *fAPAR* can be made using two *PAR* sensors to resolve both incident and reflected *PAR*. In benthic environments, *PAR* absorbance typically is above 80 % of incident near-bed irradiance in sedimentary habitats and approaches 100 % in habitats with greater structural complexity (higher light scattering) such as in seagrass beds (Al-Najjar et al., 2012;Zimmerman, 2003). Therefore, while it is advisable (and feasible) to quantify both incident and reflected *PAR* throughout the EC

10 deployment for *LUE* estimates, assuming *fAPAR* = 1.0 is expected to only induce a slight bias (underestimate) to the *LUE*. Since *fAPAR* was not measured in the studies by Attard et al. (2014) and Attard et al (in review), this study assumes *fAPAR* = 1.0. To test the validity of this assumption, direct measurements of *fAPAR* were made on a separate occasion at a site with bare sediments in Oslofjord in Norway in July 2019. Here, two cross-calibrated high-quality cosine *PAR* sensors (a Biospherical QCP-

15 2000 and a Li-cor LI-192) were affixed to a frame and placed on the seafloor at a water depth of 8 m, with the sensors located 0.5 m above the seabed. The sensors logged incident and reflected *PAR* (µmol photons m^{-2} s^{-1}) every minute over 3 days.

2.3.2 Computing hourly and daily light-use efficiency (LUE)

Once the best method for computing *GPP* was identified, hourly *GPP* was converted from units of

20 mmol O$_2$ m^{-2} h^{-1} to µmol O$_2$ m^{-2} s^{-1} and the hourly *LUE* was computed as $LUE_{hourly} = GPP_{hourly}/$ $PAR_{hourly} * fAPAR$, with units of O$_2$ photon^{-1}. Similarly, daily *GPP* (mmol O$_2$ m^{-2} d^{-1}), computed as

$GPP = FLUX_{day} + \left|\overline{FLUX_{night}}\right|$, and daily integrated PAR (mmol photon m^{-2} d^{-1}) were used to compute daily LUE (O$_2$ photon^{-1}) as $LUE_{daily} = GPP_{daily}/PAR_{daily} * fAPAR$.

3. Results and Discussion

3.1 Hourly *GPP* and light-saturation curves

In the four-day dataset from Greenland (Attard et al., 2014), hourly GPP ranged from 0 to 8 mmol O$_2$ m^{-2} h^{-1} under maximum daytime irradiance of up to 400 µmol photons m^{-2} s^{-1}. Hourly GPP measured in the first half of the day were very similar to rates resolved in the second half of the day under similar PAR intensities, indicating no substantial flux hysteresis (Fig. 1). Hourly GPP showed a tight correlation with seabed PAR, with R^2 values for the light-saturation curves ranging from 0.83 to 0.93 (Fig. 1). Overall, the highest R^2 values for the light-saturation curves for this dataset were achieved using a static daytime R rate which was defined as an average of all night-time fluxes ($|\overline{N_1 + N_2}|$). This approach achieved R^2 values in the light-saturation curves that were up to 10 % higher than when R was defined using the first night-time period alone ($|\overline{N_1}|$).

In the EC dataset from the Baltic Sea, a clear hysteresis was observed in the O$_2$ fluxes. Hourly O$_2$ fluxes in the second half of the day were up to 4-fold lower than within the first half of the day under similar irradiance levels. Light-saturation curve R^2 values varied depending on the method used to define the daytime R rate (Fig. 2). In all three days from this dataset, the highest R^2 values were obtained using dynamic daytime R rates defined as either a linear or sigmoidal increase with time. These two approaches produced GPP estimates with the best quality: all hourly GPP values were positive, and the fitting parameters P_m, I_k and α had the lowest standard errors (Fig. 2). While P_m and α showed good

agreement between the four methods, static R approaches tended to overestimate the I_k since hysteretic fluxes tend to bias light-saturation curves towards linearity.

Hourly GPP computed using sigmoidal increases in daytime R for the Baltic Sea dataset ranged from 0 to 7 mmol O_2 m^{-2} h^{-1} under PAR levels of up to 350 μmol photons m^{-2} s^{-1} (Fig. 3). Light-saturation curves provided high R^2 values for day 1 and day 3 of 0.83 and 0.81. The light-saturation curve for day 2 converged to a linear fit with an R^2 of 0.94 (Fig. 3).

3.2 Light-use efficiency

Hourly LUE estimates for the two datasets indicated high LUE of up to 0.09 O_2 photon^{-1} under light-limiting conditions of < 20 µmol PAR m^{-2} s^{-1} (Fig. 4). Light-use efficiency declined quasi-exponentially with time (and PAR) to around one-tenth of the value by the middle of the day, and then it increased again towards sunset to LUE values comparable to the morning. This observation is consistent with the microsensor and benthic chamber studies by Al-Najjar et al. (2012), Brodersen et al. (2014) and Godwin et al. (2014) who document maximum LUE under light-limiting conditions and a decline in LUE under high irradiance levels typical of the middle of the day. Daily LUE estimated as the ratio between GPP_{daily} and PAR_{daily} (both in mmol mm^{-2} d^{-1}) ranged from 0.008 to 0.013 O_2 photon^{-1} in Greenland and was 0.006 to 0.007 O_2 photon^{-1} in the mussel bed dataset from the Baltic Sea (Fig. 5). This indicates that the soft sediment habitat in Greenland had higher photosynthetic efficiency than the rocky mussel bed in the Baltic Sea on a daily timescale for the investigated data. However, in all cases daily LUE is ~ an order of magnitude or lower than the theoretical maximum of 0.125 O_2 photon^{-1}.

The LUE values presented in this study are expected to be underestimated due to the assumption of $fAPAR = 1.0$ (i.e. by assuming that all incident PAR is absorbed by the seabed). A fraction of the
incoming irradiance is reflected and thus is not available for photosynthesis. Reflected *PAR* ranged from 17.5 % to 1.9 % in the study on microbial mats by Al-Najjar et al. (2012) and was up to 12 % in the coral symbiont study by Brodersen et al. (2014). Direct measurements of *fAPAR* were not available for the datasets used in this study, but measurements from a bare sediments site in Oslofjord indicated reflected *PAR* on the order of 8-10 % (Fig. 6). It is therefore likely that the *LUE* estimates presented in this study are underestimated by ~10 %.

4. Conclusion

A key requirement of the *LUE* approach is high-quality *GPP* data. Despite there being numerous potential obstacles to obtaining this data (Table 1), a growing number of eddy covariance studies document tight relationships between hourly fluxes and sunlight availability in a wide array of aquatic habitats such as in sediment deposits, seagrass canopies, coralline algal beds and coral reefs (Berg et al., 2013;Chipman et al., 2016;Attard et al., 2014;Attard et al., 2015;Rheuban et al., 2014;Long et al., 2013;Long et al., 2015;Koopmans et al., 2020;Rovelli et al., 2017). In this study, R^2 values for light-saturation curves ranged from 0.83 to 0.94 indicating a predominant primary production signal, and this gives credence to applying the *LUE* approach.

Constraining the daytime *R* rate on an hourly timescale is clearly a challenge, especially on the spatial scales included within eddy covariance measurements. Assuming a linear or sigmoidal increase in *R* with time is consistent with observations of accumulating leached photosynthates such as carbohydrates that stimulate daytime *R* (de Winder et al., 1999;Epping and Jørgensen, 1996); however, more experimental data are required to investigate these assumptions in detail. The theoretical maximum *LUE* of 0.125 O_2 photon^{-1} provides an upper constraint on the *GPP* that is possible for given *PAR* level.

Hourly *LUE* at the start and at the end of the day often approached the theoretical maximum (Fig. 4), so it is unlikely that the *GPP* rates in these datasets were substantially underestimated.

Light-saturation curves are a useful tool to evaluate flux hysteresis and ways to correct for this. There are several considerations when computing hourly *GPP* that will influence both the R^2 value as well as the fitting parameters P_m, α and I_k. Since these parameters hold real-world significance (i.e. they are not just operators within the mathematical expression; Jassby and Platt (1976)) it is important to consider factors that may introduce bias.

Overall, the *LUE* approach provides a useful means to compare photosynthetic performance of submerged habitats on hourly and daily timescales. This provides opportunities to generate hypotheses about the importance of habitat structure (e.g. organization of photosynthetic elements) and energy flow. In terrestrial environments, this approach has been used to investigate the effects of biodiversity and biodiversity loss on habitat productivity. Similar analyses ported to the aquatic realm would constitute timely studies.

5. Data availability

The hourly PAR and eddy covariance fluxes required to generate these datasets will be made openly available in a FAIR-aligned data repository upon acceptance of the manuscript.

6. Author contribution

5 KMA conceived the idea, collected the data and processed the data. KMA wrote the manuscript with input from RNG.

7. Acknowledgements

We are grateful to our colleagues at the Greenland Climate Research Centre in Nuuk, Greenland, and at the Tvärminne Zoological Station in Finland for their help with fieldwork. This work was supported by

10 the Walter and Andreé de Nottbeck Foundation, the Academy of Finland (grant agreement numbers 283417 and 294853), and Denmark's Independent Research Fund (FNU 7014-00078).

8. References

Adams, M. P., Ferguson, A. J. P., Maxwell, P. S., Lawson, B. A. J., Samper-Villarreal, J., and O'Brien, K. R.: Light history-dependent respiration explains the hysteresis in the daily ecosystem metabolism of seagrass, Hydrobiologia, 766, 75-88, 10.1007/s10750-015-2444-5, 2016.

5 Al-Najjar, M. A. A., de Beer, D., Jørgensen, B. B., Kühl, M., and Polerecky, L.: Conversion and conservation of light energy in a photosynthetic microbial mat ecosystem, The ISME Journal, 4, 440-449, 10.1038/ismej.2009.121, 2010.

Al-Najjar, M. A. A., de Beer, D., Kühl, M., and Polerecky, L.: Light utilization efficiency in photosynthetic microbial mats, Environ Microbiol, 14, 982-992, 10.1111/j.1462-2920.2011.02676.x, 2012.

Attard, K. M., Glud, R. N., McGinnis, D. F., and Rysgaard, S.: Seasonal rates of benthic primary production in a Greenland
10 fjord measured by aquatic eddy correlation, Limnol Oceanogr, 59, 1555-1569, 10.4319/lo.2014.59.5.1555, 2014.

Attard, K. M., Stahl, H., Kamenos, N. A., Turner, G., Burdett, H. L., and Glud, R. N.: Benthic oxygen exchange in a live coralline algal bed and an adjacent sandy habitat: an eddy covariance study, Marine Ecology Progress Series, 535, 99-115, 10.3354/meps11413, 2015.

Attard, K. M., Hancke, K., Sejr, M. K., and Glud, R. N.: Benthic primary production and mineralization in a High Arctic
15 fjord: in situ assessments by aquatic eddy covariance, Marine Ecology Progress Series, 554, 35-50, 10.3354/meps11780, 2016.

Attard, K. M., Rodil, I. F., Berg, P., Norkko, J., Norkko, A., and Glud, R. N.: Seasonal metabolism and carbon export potential of a key coastal habitat: The perennial canopy-forming macroalga *Fucus vesiculosus*, Limnol Oceanogr, 64, 149-164, 10.1002/lno.11026, 2019a.

20 Attard, K. M., Rodil, I. F., Glud, R. N., Berg, P., Norkko, J., and Norkko, A.: Seasonal ecosystem metabolism across shallow benthic habitats measured by aquatic eddy covariance, Limnology and Oceanography Letters, 4, 79-86, 10.1002/lol2.10107, 2019b.

Berg, P., Røy, H., and Wiberg, P. L.: Eddy correlation flux measurements: the sediment surface area that contributes to the flux, Limnol Oceanogr, 52, 1672-1684, 10.4319/lo.2007.52.4.1672, 2007.

25 Berg, P., Glud, R. N., Hume, A., Stahl, H., Oguri, K., Meyer, V., and Kitazato, H.: Eddy correlation measurements of oxygen uptake in deep ocean sediments, Limnol Oceanogr-Meth, 7, 576-584, DOI 10.4319/lom.2009.7.576, 2009.

Berg, P., Long, M. H., Huettel, M., Rheuban, J. E., McGlathery, K. J., Howarth, R. W., Foreman, K. H., Giblin, A. E., and Marino, R.: Eddy correlation measurements of oxygen fluxes in permeable sediments exposed to varying current flow and light, Limnol Oceanogr, 58, 1329-1343, 10.4319/lo.2013.58.4.1329, 2013.

30 Berg, P., Reimers, C. E., Rosman, J. H., Huettel, M., Delgard, M. L., Reidenbach, M. A., and Ozkan-Haller, H. T.: Technical note: Time lag correction of aquatic eddy covariance data measured in the presence of waves, Biogeosciences, 12, 6721-6735, 2015.

Berg, P., Delgard, M. L., Glud, R. N., Huettel, M., Reimers, C. E., and Pace, M. L.: Non-invasive flux Measurements at the Benthic Interface: The Aquatic Eddy Covariance Technique, Limnology and Oceanography e-Lectures, 7, 1-50,
35 10.1002/loe2.10005, 2017.

Brand, A., McGinnis, D. F., Wehrli, B., and Wuest, A.: Intermittent oxygen flux from the interior into the bottom boundary of lakes as observed by eddy correlation, Limnol Oceanogr, 53, 1997-2006, DOI 10.4319/lo.2008.53.5.1997, 2008.

Brodersen, K. E., Lichtenberg, M., Ralph, P. J., Kühl, M., and Wangpraseurt, D.: Radiative energy budget reveals high photosynthetic efficiency in symbiont-bearing corals, Journal of The Royal Society Interface, 11, 20130997,
40 doi:10.1098/rsif.2013.0997, 2014.

Chipman, L., Berg, P., and Huettel, M.: Benthic Oxygen Fluxes Measured by Eddy Covariance in Permeable Gulf of Mexico Shallow-Water Sands, Aquatic Geochemistry, 10.1007/s10498-016-9305-3, 2016.

Cook, P. L. M., Wenzhofer, F., Glud, R. N., Janssen, F., and Huettel, M.: Benthic solute exchange and carbon mineralization in two shallow subtidal sandy sediments: Effect of advective pore-water exchange, Limnol Oceanogr, 52, 1943-1963, DOI
45 10.4319/lo.2007.52.5.1943, 2007.

de Winder, B., Staats, N., Stal, L. J., and Paterson, D. M.: Carbohydrate secretion by phototrophic communities in tidal sediments, Journal of Sea Research, 42, 131-146, https://doi.org/10.1016/S1385-1101(99)00021-0, 1999.

Donis, D., McGinnis, D. F., Holtappels, M., Felden, J., and Wenzhoefer, F.: Assessing benthic oxygen fluxes in oligotrophic deep sea sediments (HAUSGARTEN observatory), Deep-Sea Res Pt I, 111, 1-10, 10.1016/j.dsr.2015.11.007, 2016.

Elser, J. J., Bracken, M. E. S., Cleland, E. E., Gruner, D. S., Harpole, W. S., Hillebrand, H., Ngai, J. T., Seabloom, E. W., Shurin, J. B., and Smith, J. E.: Global analysis of nitrogen and phosphorus limitation of primary producers in freshwater, marine and terrestrial ecosystems, Ecol Lett, 10, 1135-1142, 10.1111/j.1461-0248.2007.01113.x, 2007.

Epping, E. H. G., and Jørgensen, B. B.: Light-enhanced oxygen respiration in benthic phototrophic communities, Marine

5 Ecology Progress Series, 139, 193-203, 1996.

Fenchel, T., and Glud, R. N.: Benthic primary production and O2-CO2 dynamics in a shallow-water sediment: Spatial and temporal heterogeneity, Ophelia, 53, 159-171, 2000.

Godwin, S. C., Jones, S. E., Weidel, B. C., and Solomon, C. T.: Dissolved organic carbon concentration controls benthic primary production: Results from in situ chambers in north-temperate lakes, Limnol Oceanogr, 59, 2112-2120,

10 10.4319/lo.2014.59.6.2112, 2014.

Hemes, K. S., Verfaillie, J., and Baldocchi, D. D.: Wildfire-Smoke Aerosols Lead to Increased Light Use Efficiency Among Agricultural and Restored Wetland Land Uses in California's Central Valley, Journal of Geophysical Research: Biogeosciences, 125, e2019JG005380, 10.1029/2019jg005380, 2020.

Holtappels, M., Glud, R. N., Donis, D., Liu, B., Hume, A., Wenzhöfer, F., and Kuypers, M. M. M.: Effects of transient

15 bottom water currents and oxygen concentrations on benthic exchange rates as assessed by eddy correlation measurements, Journal of Geophysical Research: Oceans, 118, 1157-1169, 10.1002/jgrc.20112, 2013.

Holtappels, M., Noss, C., Hancke, K., Cathalot, C., McGinnis, D. F., Lorke, A., and Glud, R. N.: Aquatic eddy correlation: quantifying the artificial flux caused by stirring-sensitive O_2 sensors, Plos One, 10, e0116564, 10.1371/journal.pone.0116564, 2015.

20 Hotchkiss, E. R., and Hall, R. O., Jr.: High rates of daytime respiration in three streams: Use of δ18OO2 and O2 to model diel ecosystem metabolism, Limnol Oceanogr, 59, 798-810, 10.4319/lo.2014.59.3.0798, 2014.

Hume, A. C., Berg, P., and McGlathery, K. J.: Dissolved oxygen fluxes and ecosystem metabolism in an eelgrass (*Zostera marina*) meadow measured with the eddy correlation technique, Limnol Oceanogr, 56, 86-96, 10.4319/lo.2011.56.1.0086, 2011.

25 Jassby, A. D., and Platt, T.: Mathematical formulation of the relationship between photosynthesis and light for phytoplankton, Limnol Oceanogr, 21, 540-547, 10.4319/lo.1976.21.4.0540, 1976.

Koopmans, D., Holtappels, M., Chennu, A., Weber, M., and de Beer, D.: High Net Primary Production of Mediterranean Seagrass (Posidonia oceanica) Meadows Determined With Aquatic Eddy Covariance, Frontiers in Marine Science, 7, 10.3389/fmars.2020.00118, 2020.

30 Kuhl, M., Glud, R. N., Ploug, H., and Ramsing, N. B.: Microenvironmental control of photosynthesis and photosynthesis-coupled respiration in an epilithic cyanobacterial biofilm, J Phycol, 32, 799-812, DOI 10.1111/j.0022-3646.1996.00799.x, 1996.

Long, M. H., Berg, P., de Beer, D., and Zieman, J. C.: *In situ* coral reef oxygen metabolism: An eddy correlation study, Plos One, 8, ARTN e58581

35 DOI 10.1371/journal.pone.0058581, 2013.

Long, M. H., Berg, P., McGlathery, K. J., and Zieman, J. C.: Sub-tropical seagrass ecosystem metabolism measured by eddy covariance, Marine Ecology Progress Series, 529, 75-90, 10.3354/meps11314, 2015.

Long, M. H., Sutherland, K., Wankel, S. D., Burdige, D. J., and Zimmerman, R. C.: Ebullition of oxygen from seagrasses under supersaturated conditions, Limnol Oceanogr, 65, 314-324, 10.1002/lno.11299, 2020.

40 McGinnis, D. F., Berg, P., Brand, A., Lorrai, C., Edmonds, T. J., and Wüest, A.: Measurements of eddy correlation oxygen fluxes in shallow freshwaters: Towards routine applications and analysis, Geophysical Research Letters, 35, 10.1029/2007gl032747, 2008.

McGinnis, D. F., Cherednichenko, S., Sommer, S., Berg, P., Rovelli, L., Schwarz, R., Glud, R. N., and Linke, P.: Simple, robust eddy correlation amplifier for aquatic dissolved oxygen and hydrogen sulfide flux measurements, Limnol Oceanogr-

45 Meth, 9, 340-347, 10.4319/lom.2011.9.340, 2011.

McGinnis, D. F., Sommer, S., Lorke, A., Glud, R. N., and Linke, P.: Quantifying tidally driven benthic oxygen exchange across permeable sediments: an aquatic eddy correlation study, Journal of Geophysical Research: Oceans, 119, 6918-6932, 10.1002/2014jc010303, 2014.

Monteith, J. L., Moss, C. J., Cooke, G. W., Pirie, N. W., and Bell, G. D. H.: Climate and the efficiency of crop production in Britain, Philosophical Transactions of the Royal Society of London. B, Biological Sciences, 281, 277-294, doi:10.1098/rstb.1977.0140, 1977.

Platt, T., Gallegos, C. L., and Harrison, W. G.: Photoinhibition of photosynthesis in natural assemblages of marine
5   phytoplankton, J Mar Res, 38, 687-701, 1980.

Ralph, P. J., Polk, S. M., Moore, K. A., Orth, R. J., and Smith, W. O.: Operation of the xanthophyll cycle in the seagrass Zostera marina in response to variable irradiance, Journal of Experimental Marine Biology and Ecology, 271, 189-207, https://doi.org/10.1016/S0022-0981(02)00047-3, 2002.

Reimers, C. E., Özkan-Haller, H. T., Albright, A. T., and Berg, P.: Microelectrode Velocity Effects and Aquatic Eddy
10 Covariance Measurements under Waves, J Atmos Ocean Tech, 33, 263-282, 10.1175/jtech-d-15-0041.1, 2016.

Rheuban, J. E., Berg, P., and McGlathery, K. J.: Multiple timescale processes drive ecosystem metabolism in eelgrass (*Zostera marina*) meadows, Marine Ecology Progress Series, 507, 1-13, 10.3354/meps10843, 2014.

Rovelli, L., Attard, K. M., Binley, A., Heppell, C. M., Stahl, H., Trimmer, M., and Glud, R. N.: Reach-scale river metabolism across contrasting sub-catchment geologies: Effect of light and hydrology, Limnol Oceanogr, 62, S381-S399,
15 10.1002/lno.10619, 2017.

Stocker, B. D., Zscheischler, J., Keenan, T. F., Prentice, I. C., Peñuelas, J., and Seneviratne, S. I.: Quantifying soil moisture impacts on light use efficiency across biomes, New Phytologist, 218, 1430-1449, 10.1111/nph.15123, 2018.

Toussaint, F., Rabouille, C., Cathalot, C., Bombled, B., Abchiche, A., Aouji, O., Buchholtz, G., Clemençon, A., Geyskens, N., Répécaud, M., Pairaud, I., Verney, R., and Tisnérat-Laborde, N.: A new device to follow temporal variations of oxygen
20 demand in deltaic sediments: the LSCE benthic station, Limnology and Oceanography: Methods, 12, 729-741, 10.4319/lom.2014.12.729, 2014.

Volaric, M. P., Berg, P., and Reidenbach, M. A.: Oxygen metabolism of intertidal oyster reefs measured by aquatic eddy covariance, Marine Ecology Progress Series, 599, 75-91, 10.3354/meps12627, 2018.

Wenzhofer, F., and Glud, R. N.: Small-scale spatial and temporal variability in coastal benthic O-2 dynamics: Effects of
25 fauna activity, Limnol Oceanogr, 49, 1471-1481, 2004.

Zimmerman, R. C.: A biooptical model of irradiance distribution and photosynthesis in seagrass canopies, Limnol Oceanogr, 48, 568-585, 10.4319/lo.2003.48.1_part_2.0568, 2003.

Table 1: Sources of EC flux variability can be broadly grouped into two categories: (1) sources that bias the measured EC flux away from the 'true' benthic flux (i.e. when EC O_2 flux ≠ benthic O_2 flux) and (2) 'true' temporal variability in the benthic O_2 exchange rate (i.e. when EC O_2 flux = benthic O_2 flux)

EC O_2 flux ≠ benthic O_2 flux	Reference	EC O_2 flux = benthic O_2 flux	Reference
Non steady-state conditions within the benthic boundary layer	(Holtappels et al., 2013;Brand et al., 2008)	Changes in diffusive boundary layer thickness in cohesive sediments	(Kuhl et al., 1996)
Sensor stirring sensitivity	(Holtappels et al., 2015)	Pore-water advection in permeable sediments	(Cook et al., 2007;McGinnis et al., 2014)
Surface wave influence	(Berg et al., 2015;Reimers et al., 2016)	Diel fauna activity	(Wenzhofer and Glud, 2004)
Sensor response time	(McGinnis et al., 2008;Berg et al., 2015)	Sediment resuspension	(Toussaint et al., 2014), Camillini et al. In review
Internal plant O_2 storage, canopy storage, or bubbling	(Attard et al., 2019a;Rheuban et al., 2014;Long et al., 2020)	Oxidation of anaerobic metabolites in sediments	(Fenchel and Glud, 2000)
		Nutrient availability	(Elser et al., 2007)
		Photosynthesis-coupled respiration	(Epping and Jørgensen, 1996)
		Acclimation of the photosynthetic system	(Ralph et al., 2002)
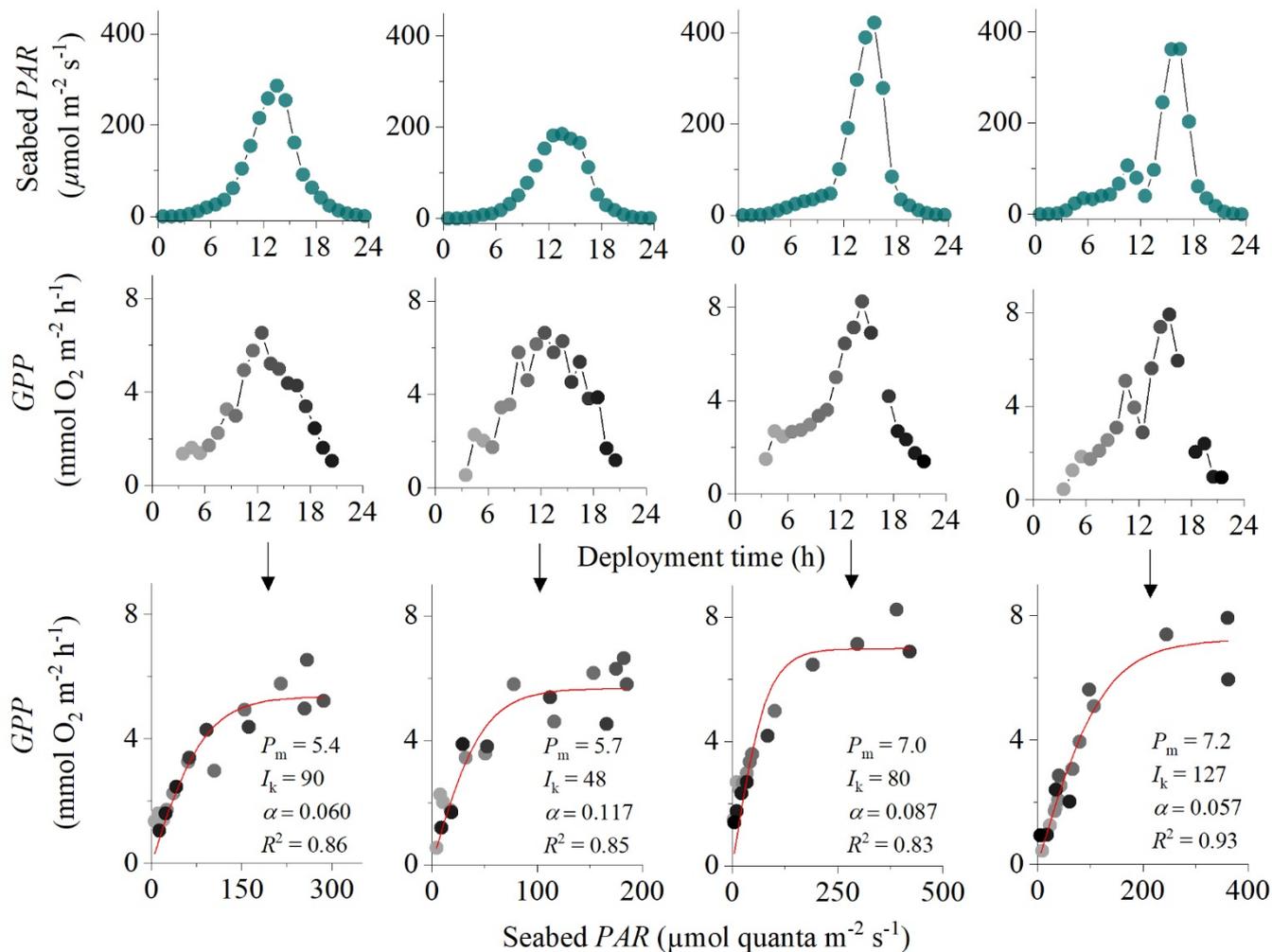
Fig. 1: Eddy covariance data measured over four consecutive days in Greenland showing seabed PAR (top panels), hourly *GPP* (middle panels) and corresponding light-saturation curves (bottom panels). Symbols in the middle and bottom panels are colour-mapped by h of day. Light-saturation curves are fitted to the data showing the maximum rate of *GPP* (P_m, mmol O_2 m^{-2} h^{-1}), the photoadaptation parameter I_k (μmol PAR m^{-2} s^{-1}), the initial slope of the curve α, and the coefficient of determination (R^2). Data modified from Attard et al. (2014).
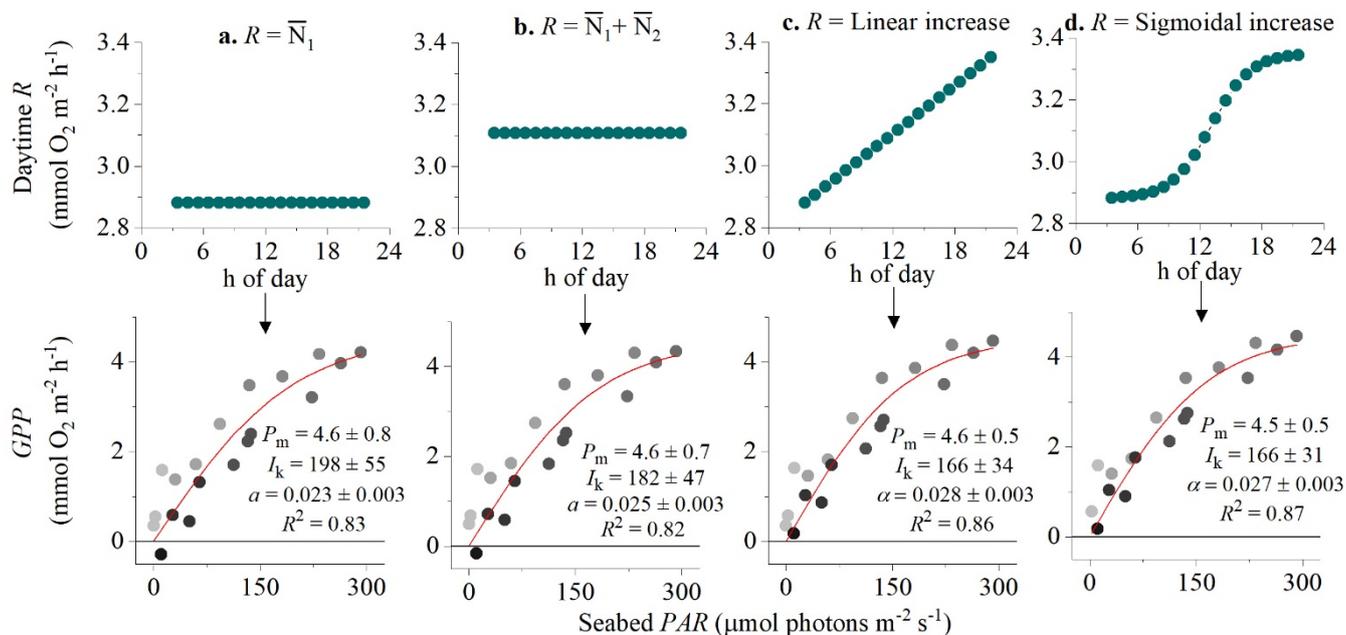
Fig. 2: Different approaches for defining the R rate during the day (and therefore the hourly GPP) from eddy covariance fluxes showing hysteresis: (a) R = average flux for the first night-time period (N_1), (b) R = average flux for both night-time periods N_1 and N_2, (c) R increases linearly from N_1 to N_2, and (d) R increases from N_1 to N_2 following a sigmoidal curve.
5   Bottom panels show corresponding light-saturation curves and fitting parameters for the maximum rate of GPP (P_m, mmol O_2 m^{-2} h^{-1}), the photoadaptation parameter I_k (μmol PAR m^{-2} s^{-1}), the initial slope of the curve α, and the coefficient of determination (R^2). Symbols in bottom panels are colour-mapped by h of day. Data modified from Attard et al. (in review).
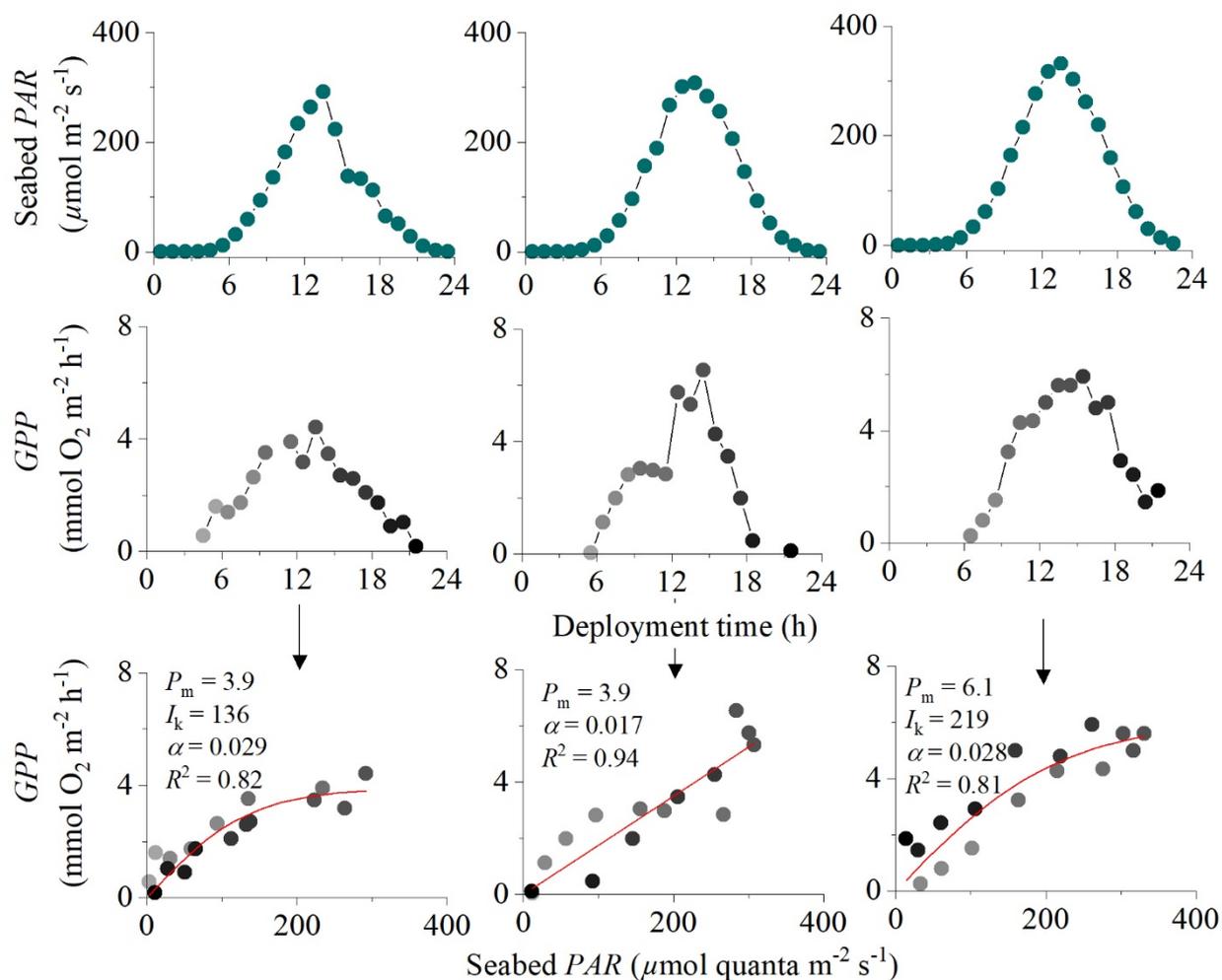
Fig. 3: Eddy covariance data measured over three consecutive days in the Baltic Sea showing seabed *PAR* (top panels), hourly *GPP* (middle panels) and corresponding light-saturation curves (bottom panels). Symbols in the middle and bottom panels are colour-mapped by h of day. Light-saturation curves are fitted to the data showing the maximum rate of *GPP* (P_m, mmol O_2 m^{-2} h^{-1}), the photoadaptation parameter I_k (μmol PAR m^{-2} s^{-1}), the initial slope of the curve α, and the coefficient of determination (R^2). Data modified from Attard et al. (in review).
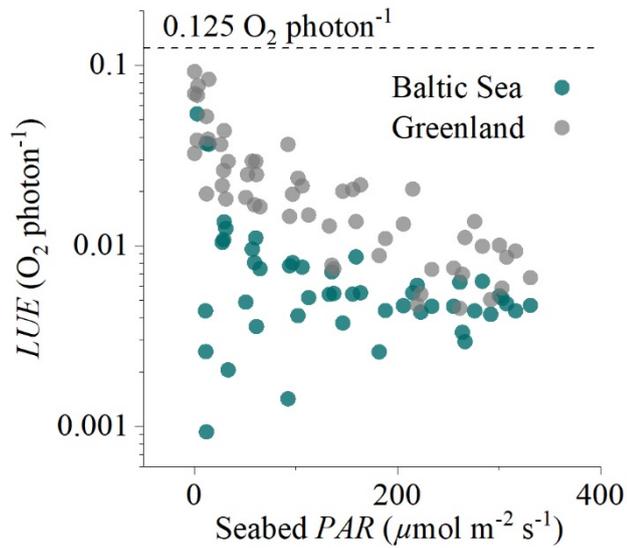
Fig. 4: Hourly light-use efficiency (*LUE*, log-axis) plotted against incoming irradiance (seabed *PAR*) for the two eddy flux datasets collected in Greenland and the Baltic Sea. The broken line indicates the theoretical maximum of 0.125 O_2 photon $^{-1}$.
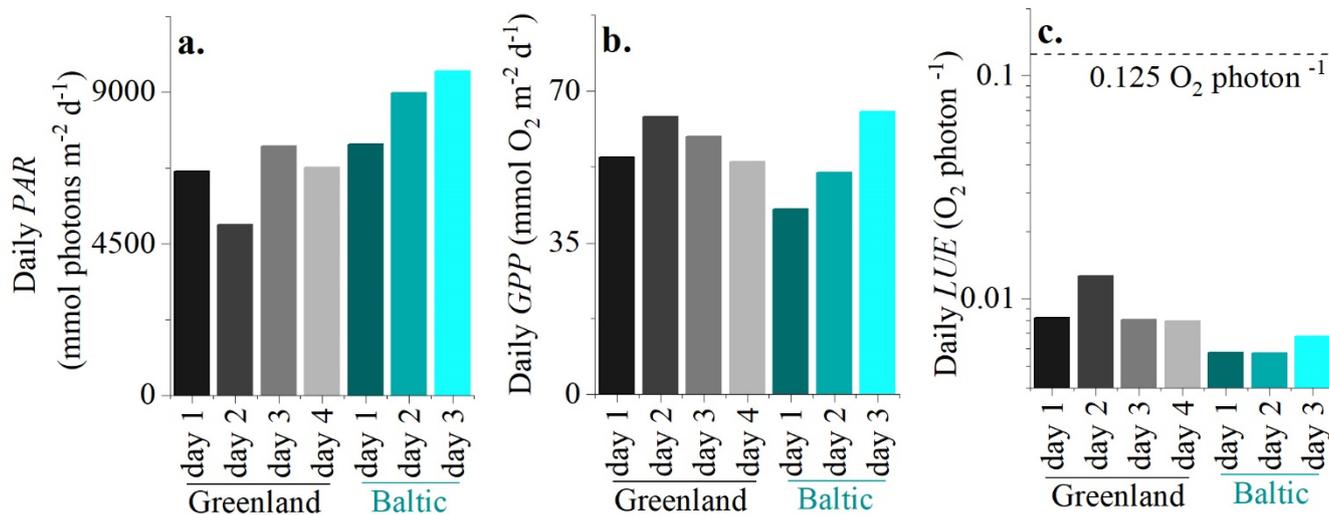
Fig. 5: (a) Daily seabed *PAR*, (b) daily benthic *GPP*, and (c) daily *LUE*. The broken line in (c) indicates the theoretical maximum of 0.125 O_2 photon $^{-1}$.
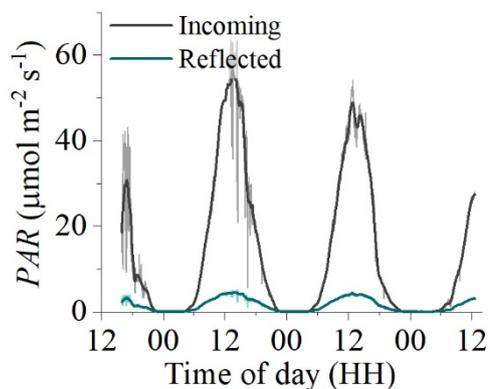
Fig. 6: Measurements of incident and reflected seabed *PAR* made using two cosine *PAR* sensors over a habitat with bare sediments at 8 m depth in Oslofjord in July 2019. Reflected *PAR* was typically 8-10 % of incident *PAR*, indicating that ~90 % of incident *PAR* was absorbed by the benthos.